MODELING COLLAPSE CHIMNEY AND SPALL ZONE SETTLEMENT AS A SOURCE OF POST-SHOT SUBSIDENCE DETECTED BY SYNTHETIC APERTURE RADAR INTERFEROMETRY

William Foxall
Lawrence Livermore National Laboratory

ABSTRACT

Ground surface subsidence resulting from the March 1992 JUNCTION underground nuclear test at the Nevada Test Site (NTS) imaged by satellite synthetic aperture radar interferometry (InSAR) wholly occurred during a period of several months after the shot (Vincent et al., 1999) and after the main cavity collapse event. A significant portion of the subsidence associated with the small (less than 20 kt) GALENA and DIVIDER tests probably also occurred after the shots, although the deformation detected in these cases contains additional contributions from coseismic processes, since the radar scenes used to construct the deformation interferogram bracketed these two later events. The dimensions of the areas of subsidence resulting from all three events are too large to be solely accounted for by processes confined to the damage zone in the vicinity of the shot point or the collapse chimney. Rather, the subsidence closely corresponds to the spall dimensions predicted by Patton's (1990) empirical relationship between spall radius and yield. This suggests that gravitational settlement of damaged rock within the spall zone is an important source of post-shot subsidence, in addition to settlement of the rubble within the collapse chimney. These observations illustrate the potential power of InSAR as a tool for Comprehensive Nuclear-Test-Ban Treaty (CTBT) monitoring and on-site inspection in that the relatively broad (~100 m to 1 km) subsidence signatures resulting from small shots detonated at normal depths of burial (or even significantly overburied) are readily detectable within large geographical areas (100 km × 100 km) under favorable observing conditions. Furthermore, the present results demonstrate the flexibility of the technique in that the two routinely gathered satellite radar images used to construct the interferogram need not necessarily capture the event itself, but can cover a time period up to several months following the shot.

In order to explore the power of InSAR to discriminate underground nuclear explosions from other seismic and subsidence events, we model settlement within the chimney and spall zones as three-dimensional distributions of point volume deflation and closing tension crack sources within prescribed subsurface volumes representing the spall and collapse damage zones. We investigate the uniqueness of fitting the InSAR observations by examining the trade-offs among the spatial and strength distributions of the sources, and the overall geometries of the damage zones. Modeling constraints are based on characteristics of collapse chimneys and spall zones deduced from available *in-situ* observations at NTS and elsewhere, analysis and interpretation of near-source ground motion data, and existing results of dynamic modeling of contained underground explosions. We discuss refinements to the modeling approach based on analyses of the mechanics of settlement within damage and rubble zones taken from the fields of mining and geotechnical engineering, and examine the potential of the InSAR technique to detect and discriminate underground nuclear tests in different geological environments.

Key Words: synthetic aperture radar interferometry, detection, source identification, source parameters, modeling

Report Documentation Page

1. REPORT DATE **SEP 2000**	2. REPORT TYPE	3. DATES COVERED **00-00-2000 to 00-00-2000**

4. TITLE AND SUBTITLE		5a. CONTRACT NUMBER
Modeling Collapse Chimney And Spall Zone Settlement As A Source Of Post-Shot Subsidence Detected By Synthetic Aperture Radar Interferometry		5b. GRANT NUMBER
		5c. PROGRAM ELEMENT NUMBER
6. AUTHOR(S)		5d. PROJECT NUMBER
		5e. TASK NUMBER
		5f. WORK UNIT NUMBER
7. PERFORMING ORGANIZATION NAME(S) AND ADDRESS(ES) **Lawrence Livermore National Laboratory,Livermore,CA,94551**		8. PERFORMING ORGANIZATION REPORT NUMBER
9. SPONSORING/MONITORING AGENCY NAME(S) AND ADDRESS(ES)		10. SPONSOR/MONITOR'S ACRONYM(S)
		11. SPONSOR/MONITOR'S REPORT NUMBER(S)

12. DISTRIBUTION/AVAILABILITY STATEMENT
Approved for public release; distribution unlimited

13. SUPPLEMENTARY NOTES
Proceedings of the 22nd Annual DoD/DOE Seismic Research Symposium: Planning for Verification of and Compliance with the Comprehensive Nuclear-Test-Ban Treaty (CTBT) held in New Orleans, Louisiana on September 13-15, 2000, U.S. Government or Federal Rights.

14. ABSTRACT
See Report

15. SUBJECT TERMS

16. SECURITY CLASSIFICATION OF:			17. LIMITATION OF ABSTRACT	18. NUMBER OF PAGES	19a. NAME OF RESPONSIBLE PERSON
a. REPORT **unclassified**	b. ABSTRACT **unclassified**	c. THIS PAGE **unclassified**	**Same as Report (SAR)**	**8**	

OBJECTIVE

Synthetic aperture radar interferometry (InSAR) imaged ground surface deformation resulting from the March 1992 JUNCTION (m_b5.6) underground nuclear test at the Nevada Test Site (NTS) that occurred over a time interval of months to years, beginning about one month after the event and the collapse of the explosion cavity (Vincent et al., 1999). A significant part of the imaged deformation associated with the Yucca Flat shots GALENA (m_b3.9) and DIVIDER (m_b4.4) most likely also occurred after the events, although in these cases the deformation contains contributions from coseismic and immediate post-shot processes (including cavity collapse and cratering), since the radar scenes used to construct the interferogram bracket the times of the shots. These observations have important implications for the potential of InSAR as a tool for monitoring a Comprehensive Nuclear-Test-Ban Treaty (CTBT) and to aid decision making for on-site inspections. First, the GALENA and DIVIDER observations illustrate that, at least in geological environments similar to Yucca Flat and under favorably arid observing conditions, shots in the magnitude 4 range can be detected, even when, as in these cases, the shots are overburied; second, the deformation signatures enable the shots to be located with an accuracy of a few tens of meters within the large (100 km x 100 km) area covered by a single interferogram; and third, the radar orbits do not necessarily need to capture the shot itself but can be collected up to several months or years after the event, which should prove particularly useful for on-site inspection.

The objective of our research is to develop techniques for inverting InSAR data to characterize underground nuclear tests and to discriminate them from other seismic events. In order to achieve this we first need to construct simple yet viable mechanical models of the sources of the observed deformation caused by well-characterized underground tests at NTS. We can then devise optimal inversion methods that can be applied in the wide variety of geological environments likely to be encountered in CTBT applications. The InSAR data themselves suggest that gravitational settlement within the near-surface spall zone and collapse chimney is the predominant source of long-term post-shot subsidence. In the work described here we conduct elastic modeling of the JUNCTION data to identify the parameters of a settlement source that will control the inversion problem, and examine available constraints on those parameters.

RESEARCH ACCOMPLISHED

InSAR Data

JUNCTION was detonated on 3/26/92 at a depth of 622 m, and was the last nuclear test to be carried out beneath Paute Mesa. Cavity collapse occurred 29 hours after the shot. The collapse chimney did not propagate to the surface, so a crater did not form. Processing of ERS-1 satellite synthetic aperture radar (SAR) data to produce interferograms that image ground deformation at NTS over two time periods, 4/24/92-6/18/93 and 4/24/92-5/26/96, is described fully in Vincent et al. (1999), and the data used here are taken from that study. Figure 1 shows the portion of the 4/24/92-6/18/93 interferogram that images deformation associated with JUNCTION. Since the shot occurred about 1 month before the beginning of the imaging interval, the interferogram captures deformation that occurred only after the event. Each fringe (one color cycle) on the interferogram corresponds to 28 mm of change in path length (range) between the radar and the ground caused by surface deformation. Figure 2 shows displacement (unwrapped phase) cross sections along the major and minor axes of the approximately elliptical deformation pattern. Construction of the cross sections assumes that the range change corresponds entirely to vertical deformation. Figures 1 and 2 show an elliptically shaped subsidence bowl having semi-major and -minor axes of approximately 1.2 and 0.9 km, respectively, and a maximum depth of about 8 cm. The full interferogram reveals deformation signatures coincident with all Paute Mesa tests since 1990, which implies that subsidence resulting from each shot occurs continuously over a period of several years.
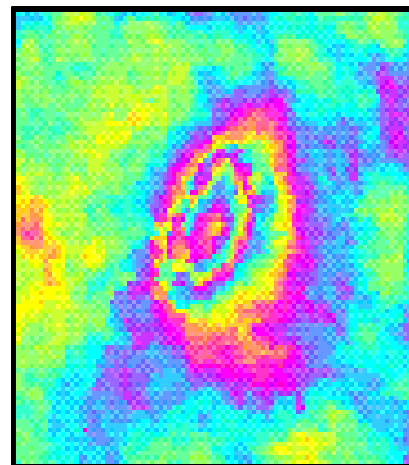

Figure 1: 4/24/92-6/18/93 interferogram imaging ground deformation associated with the JUNCTION event.
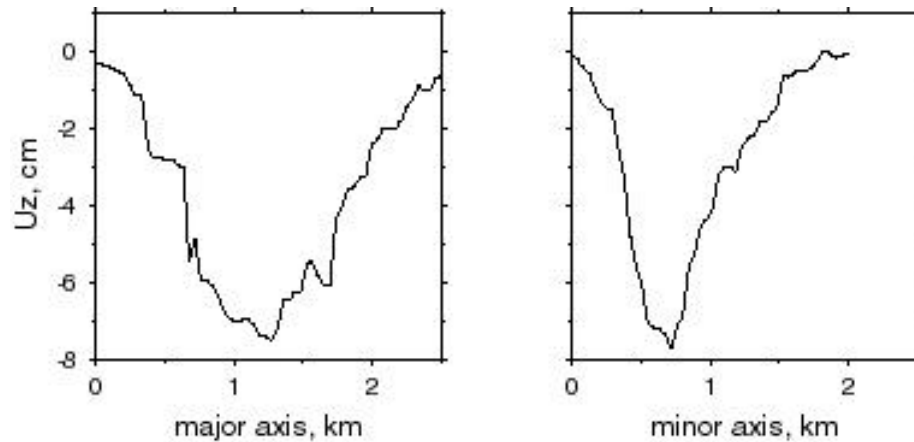
Figure 2: Vertical displacement cross sections (unwrapped phase) along the major and minor axes of the interferogram in Figure 1.

Subsidence Source Models

The most obvious potential source of subsidence following an underground explosion is gravitational settlement of rubble within the collapse chimney and of the intensely fractured rock surrounding the shot point. In general, the chimney is centered on the shot point and has a maximum radius perhaps 15-20% greater than the cavity (e.g. Houser 1969). A zone of intense fracture damage is estimated to extend up to about 5 cavity radii beyond the cavity wall. A cavity radius of about 60 m is estimated for JUNCTION, based the NEIC m_b of 5.5, the m_b-yield relationship of Murphy (1996), and the yield-radius relationship of Terhune and Glenn (1977), which gives a chimney radius of less than 100 m and a damage zone radius of roughly 300 m. The damage radius, therefore, is about three times smaller than the length of the semi-minor axis of the subsidence bowl, which suggests an additional, laterally more extensive source is needed to explain the observed subsidence. The close agreement of the length of the major axis with the maximum radius of spall estimated using Patton's (1990) empirical spall radius-yield relationship for Paute Mesa events leads us to propose gravitational settlement of damaged rock within the near-surface spall zone as this additional source.

Spalling is caused by the down-going tensional wave front produced by reflection at the ground surface of the up-going compressional pulse from a buried explosion (e.g. Eisler and Chilton 1964). Tensile failure of near-surface material occurs where the tensional stress exceeds the sum of the dynamic compressional stress, the overburden and the tensile strength of the material, resulting in detachment and ballistic free-fall of the overlying layer. Spall terminates when the spalled layer falls back under gravity to impact the underlying material. Multiple spalling (Eisler et al. 1966) throughout a range of depths results in a complex spall zone that extends from a few tens of meters below the surface to a maximum depth of a few hundred meters, depending on the yield and depth of the explosion (e.g. Patton, 1990). We propose the following, at present largely heuristic model, to explain how the spall zone can become a source of subsequent subsidence.

It is seems likely that during the interval of ballistic free-fall following spall detachment at any location, rock fragments will became detached from the bottom of the spalled slab and fall back into the spall gap to form a layer of rubble; this is particularly likely considering that multiple spall itself fractures the rock over a large range of scale lengths. The rubble layer will contain significant void space owing to mismatch between the rock fragments (bulking). Bulking (bulking factor$= V_D/V$, where V_D and V are the volume of the damaged and undamaged rock, respectively) depends on a complex combination of factors, including the shape and size distributions of the fragments - which in turn depend upon the density and orientations of pre-existing fractures - and the rotation of the fragments as they fall, which depends on the width of the spall gap. Much of the newly created void space will be destroyed by compaction at slapdown, but apparently bulking is sufficient either for some of the rubble void space to survive or for yet new void space to be created by imperfect rejoin of the rock across the plane of spall failure. Slapdown itself creates new damage, which is primarily compaction of the underlying material but probably includes shear failure and associated dilatation both above and below the failure plane. Another possible source of void creation is minor spall that results in tensile opening but not in significant ballistic free fall.

We assume that following slapdown, the bulked rock within the spall zone begins to settle under gravity, reducing the void volume. The predominant deformation mechanism is likely to be low-rate, stable frictional sliding (steady-state creep) on inter-block contacts within the fractured and bulked rock mass. We expect that fluid effects involving percolation of surface water play an important role through sub-critical growth of microcracks and/or pore pressure effects. This mechanism also applies to the collapse chimney, where bulking of the chimney rubble has been relatively well studied (e.g. Houser 1969; Hakala 1970), and perhaps also to the zone of compressional damage surrounding the shot point.

Elastic Modeling

Although the mechanism of gravity driven creep outlined above is inelastic, we can simulate void closure using a spatial distribution of dislocation sources associated with a prescribed distribution of volume deflation or closing displacement. We then model the resulting surface deformation by embedding the sources in an elastic half space, under the assumption that the overburden and the spall zone itself respond elastically. For the work described here, we model void closure by point volume deflation sources distributed within a 3-D volume having a prescribed geometry that represents the overall shape of the spall zone. The point source elastic solutions are those of Okada (1992). The purpose of the present phase of modeling is to assess the viability of spall zone settlement as a source of the observed surface subsidence, to evaluate the sensitivity of the surface deformation field to the shape of the spall zone and the distribution of source strength (i.e. amount of void closure), and to examine the trade-off among these parameters. The results of previous observational and modeling studies are used to constrain the selection of model parameters within physically plausible bounds.

Spall Zone Shape

The 3-D shape of the spall zone model, shown in vertical cross-section in Figures 3b and 4b, is based on the results of dynamic 2-D finite difference modeling of the HARZER test by John Rambo (LLNL), as shown in Figure 11 of Patton (1988). Both HARZER and JUNCTION were $m_b \sim 5.5$ events. HARZER was detonated within 2 km of JUNCTION at about the same depth and in similar geology. The maximum surface range (1.2 km) of the spall zone closely agrees with the estimate from Patton's (1990) empirical relationship, but the maximum spall depth (270 m) is significantly greater. The overall bowl shape of the zone is generally similar to that reported by Stump and Reinke (1987), based on ground motion recordings of small chemical shots in alluvium, and to (unpublished) dynamic models from several other workers. The model shown in Figures 3b and 4b is built from three vertically stacked 3-D layers, each of which has the shape of an inverted elliptical cone (truncated at the apex in the case of the two upper layers). The elliptical horizontal sectional shape was chosen to match the observed deformation pattern, and is discussed further below. Figures 3b and 4b show the distribution of point sources in the layers. The volumetric moment in each layer was distributed uniformly among the point sources. The moments assigned to the layers were then adjusted relative to each other to provide the best fit to cross-sections through the data along the major and minor axes of the observed deformation pattern.

Figures 3a and 4a show the best fit to the data, obtained with a model in which 47%, 47% and 6% of the total volumetric moment of the spall zone is contained in Layers 1,2 and 3, respectively. Therefore, for the geometry constrained by the HARZER results, the model concentrates the void closure towards the center of the spall zone (surface ranges less than approximately one depth of burial [DOB]). The cumulative void closure in this model represents less than 0.1% of the total volume of the spall zone. Note that the uppermost layer is shifted +100 m and +200 m along the major and minor axes, respectively, to fit the asymmetry in the data cross sections. Figure 5 compares the fit obtained from the spall zone model with models representing 70-cm closure of a 150-m diameter void at the top of the collapse chimney (depth 300 m) and 22-cm total void closure within a 600-m diameter damage zone at 620-m depth. The amount of closure in each of the latter models was adjusted to provide the best fit to the data. The spall model produces a significantly better fit. The essential point is that a laterally extensive source with distributed, small amounts of void closure is needed to fit the width of the deformation pattern.
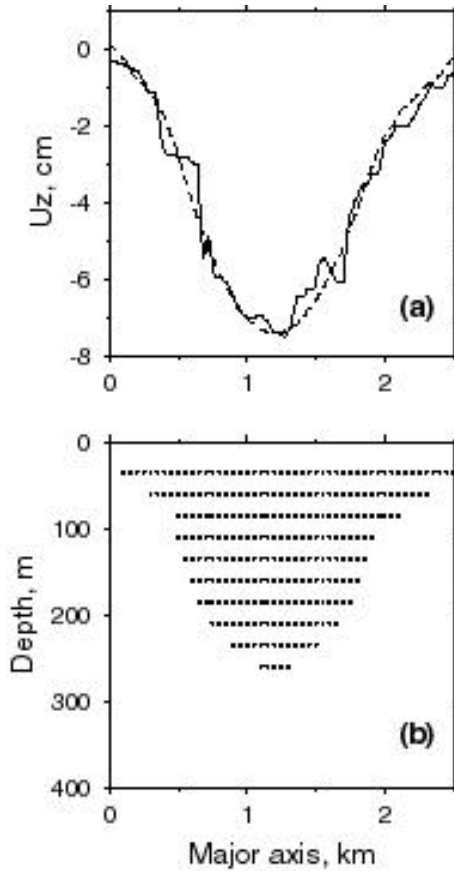
Figure 3: **(a)** Fit of vertical displacement computed (**dashed**) from 3-D spall zone source model to data (**solid**) along major axis of deformation pattern. (**b**) Major axis vertical cross section though uniform distribution of point sources.
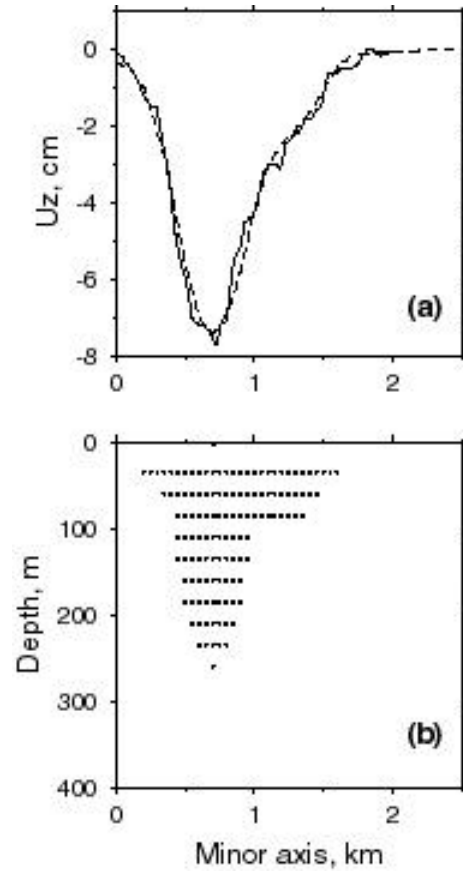
Figure 4: Same as Figure 3 for minor axis of deformation pattern
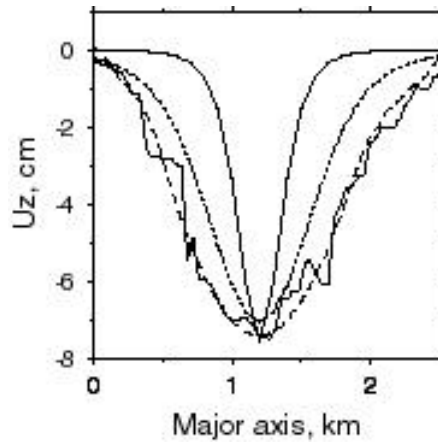

Figure 5: Comparison of data fits for 3-D spall source model (**dashed**), 70-cm closure of 150 m diameter void in collapse chimney at 300-m depth (**solid**), and 22-cm closure within 600-m-diameter damage zone at 620 m depth (**dotted**).

Distribution of Void Volume

Although the depth-integrated spall damage falls off with distance from SGZ as a result of the decreasing maximum depth of spall, it might be expected that the degree of damage would also decay with distance at any given depth. In order to test this possibility an empirical or physical basis is needed to guide the selection of appropriate types of decay laws. So far, we have found very little information about the distribution of damage in spall zones based on direct observations. Some numerical dynamic modeling has carried the calculations through the ballistic interval, but the resulting estimates of residual damage are sensitive to assumed bulking factors, which have large uncertainties. Our initial approach to this problem is based on the work of Stump and Weaver (1992), who proposed a theoretically and empirically based two-stage power law decay of peak spall velocity with distance; the ground motion decays very slowly to a surface range of about 1 DOB and much more rapidly beyond that point. According to simple ballistic theory, the width of the spall gap, $S \propto V_P^2$, where V_P is the peak spall velocity, so bulking should be related to V_P. However, as discussed above, bulking is a complex process, so the form of the relationship between bulking factor and spall velocity is not obvious. In our preliminary assessment we merely assume that void closure volume decays from a maximum at SGZ according to power laws having different exponents on either side of surface range = 1 DOB, and adjust the model to fit the data. For a source layer of given depth and shape, the input model parameters are the point source volumetric moments at SGZ, along the outer periphery of the spall zone, and at surface range = 1 DOB. Figure 6 shows the fit obtained using a single sheet of sources at a depth of 90 m. This preliminary result suggests that the fall off in depth-integrated source strength with range can be represented by a 2-D source having a spatial decay relationship. If, in fact, there is significant decay of source strength with range at constant depth, then there is a potentially strong trade-off between the geometry of the source volume and the assumed decay. Therefore, more work is needed to identify physically appropriate decay laws.
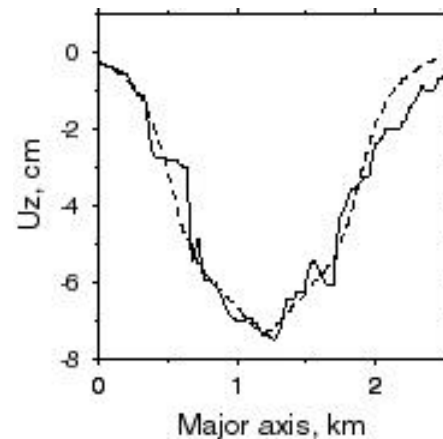

Figure 6: Fit of vertical displacement computed (**dashed**) from single sheet of point sources with two-branch power law decay to data (**solid**) along major axis of deformation pattern.

Two potential causes of the elliptical shape of the surface deformation pattern (Figure 1) are an aspherical explosive source or azimuthally dependent wave propagation effects related to near surface geologic structure. Either would produce a spall zone that is not axially symmetric. Conceivably, an aspherical source could result from the influence of the regional tectonic stress field on cavity growth and shock propagation, but to our knowledge this has not been investigated. Analysis of ground motion data from DIVIDER (Steve Taylor, LANL, unpublished manuscript) shows that nearby faults can have a major influence on spall ground motions and hence on the shape of the spall zone. Specifically, reflections from a fault plane can focus energy inwards towards SGZ and attenuate spall ground motion on the opposite side of the fault. This model appears consistent with the deformation pattern for JUNCTION, where faults striking approximately N-S are mapped 500-700 m on either side of the working point.

CONCLUSIONS AND RECOMMENDATIONS

The simple elastic modeling results presented above demonstrate that gravitational settlement of the damaged rock mass within the near surface spall zone provides a satisfactory explanation of the localized, intermediate to long-term (months to years) subsidence imaged by InSAR following NTS underground nuclear tests. Because likely alternative sources are confined to relatively short ranges around ground zero, they do not produce surface deformation that matches the dimensions of the observed subsidence patterns. In the case of the JUNCTION data analyzed here, good estimates of the shape, dimensions, and depth of the spall zone are provided by well constrained, 2-D (vertical cross-section) finite difference modeling of a nearby test that closely matches the size, depth of burial, and geologic environment of JUNCTION. We obtained a close fit to the InSAR data by extending this spall zone shape to 3-D as three layers, each having the shape of an inverted elliptical cone and a uniform

distribution of point volumetric deflation sources of equal moment. The data fit is quite sensitive to the shape and depth of the spall zone. Relatively modest perturbations to the 2-D shape and depth of the spall zone provided by the finite difference results were needed to fit the data, suggesting that these parameters of the source model can be relatively well constrained. Preliminary results on the distribution of void volume (i.e. source strength) suggest a potential trade off between the geometry of the spall zone and spatial decay of source strength, but are inconclusive. The difficulty lies in finding relations for the decay of source strength with surface range and depth that are supported by data or otherwise physically motivated.

The settlement model we propose is speculative, and detailed study of the damage mechanisms responsible for bulking and void creation in spall zones is needed to verify it. This can be approached by examination of existing dynamic modeling results that run through the slapdown phase. Estimates of bulking factors for specific rock types and geologic environments are likely to be the most uncertain parameters in these calculations. Therefore, additional modeling would probably be necessary, for which it will be important to seek constraint on bulking from the mining and geotechnical fields. A complementary approach will be to explore damage mechanics models that can provide a generalized statistical description of spall zone damage. Most importantly, in order to make the best use of InSAR data on a worldwide basis, it would be desirable to analyze available *in situ* data and modeling results from the widest possible variety of geologic environments. Three-dimensional dynamic modeling would be necessary if the non-axisymmetric shape of deformation fields like that produced by JUNCTION proves to be diagnostically useful. The fact that the net surface deformation produced by NTS explosions is predominantly subsidence might pose a discrimination challenge in that similar deformation patterns could plausibly be caused by mine collapses of similar size.

The elastic modeling presented here is only a crude representation of a complex inelastic settlement process. However, as long as the elastic representation can capture the essential features of the process, such as the cumulative loss of void volume and the equivalent elastic response of the overburden, it is just what is required as the core of a tractable and efficient inverse technique that can be applied in the variety of geological environments CTBT monitoring demands.

ACKNOWLEDGEMENT

REFERENCES

Eisler, J., and F. Chilton, (1964) Spalling of the Earth's Surface by Underground Nuclear Explosions, J. Geophys. Res., **69**, 5285-5293.

Eisler, J., F. Chilton, and F. Sauer, (1966) Multiple Subsurface Spalling by Underground Nuclear Explosions, J. Geophys. Res., **71**, 3923-3927.

Hakala, W., (1970) Subsidence Caused by an Underground Nuclear Explosion, Proc., Symposium on Engineering with Nuclear Explosives, Jan. 14-16, 1970, Las Vegas, NV, Am. Nuclear Soc./U.S. Atomic Energy Commission, 1428-1455.

Houser, F., (1969) Subsidence Related to Underground Nuclear Explosions, Nevada Test Site, Bull. Seismol. Soc. Am., **59**, 2231-2251.

Murphy, J., (1996) Types of Seismic Events and Their Source Descriptions, in Monitoring a Comprehensive Test Ban Treaty, E. Husebye and A. Dainty (eds.), Kluwer Academic Publishers, Dordrecht, 225-246.

Okada, Y., (1992) Internal Deformation Due to Shear and Tensile Faults in a Half Space, Bull. Seismol. Soc. Am., **82**, 1018-1040.

Patton, H., (1990) Characterization of Spall from Observed Strong Ground Motions on Mesa, Bull. Seismol. Soc. Am., **80**, 1326-1345.

Patton, H., (1988) Source Models of the Harzer Explosion from Regional Observations of Fundamental- and Higher-Mode Surface Waves, Bull. Seismol. Soc. Am., **78**, 1133-1157.

Stump. B. and R. Reinke, (1987) Experimental Seismology: *In situ* Source experiments, Bull. Seismol. Soc. Am., **77**, 1295-1311.

Stump, B. and T. Weaver, (1992) Physical Models of Spall Ground Motions and the Determination of Spatial Decay Rates, LAUR-92-451, Los Alamos National Laboratory.

Terhune, R and H. Glenn, (1997) Estimate of Earth Media Shear Strength at the Nevada Test Site, UCRL-52358, Lawrence Livermore National Laboratory.

Vincent, P., B. Foxall, and W. Walter, (1999) Analysis, Comparison and Modeling of Radar Interferometry Data of Surface Deformation Signals Associated with Underground Explosions, Mine Collapses and Earthquakes Phase I: Underground Explosions, Nevada Test Site, Proc. 21st Seismic Research Symposium, Las Vegas, NV, 21-24 Sep., 1999, 775-784.